Comparisons of CFD and PIV data for the flow around a rectangular cylinder

Zachary J. Taylor [a], Emanuela Palombi[a], Gregory A. Kopp [a], William J. Holmes [b]

[a] *Boundary Layer Wind Tunnel Laboratory, University of Western Ontario, London, Canada*
[b] *ANSYS Canada Ltd., Waterloo, Canada*

KEYWORDS: Particle Image Velocimetry, Computational Fluid Dynamics, Rectangular cylinder

1 INTRODUCTION

Computing power has increased substantially over the last several years. Along with developments in processing speed, the reliability of commercially available computational fluid dynamics (CFD) packages has also increased. The wind engineering community has long recognized the importance and difficulties of using CFD as a design tool [1]. The need has also been recognized to validate the results of these numerical simulations with both full scale and wind tunnel test data [2].

One of the simplest forms of a bluff body is the rectangular cylinder. Although the geometry is simple, the flow around such a body proves to be quite complicated and difficult to predict because of the separation at the leading edge, subsequent reattachment, and separation again at the trailing edge. Compounding this difficulty are possible interactions between vortices shed from the leading edge interacting with vortices shed from the trailing edge. Thus, this flow has many of the characteristics which make computation difficult in bluff body aerodynamics. There has been some work done to understand this flow [3,4]; however, there remains a need for research in order to develop algorithms for the numerical prediction of long-span bridge aerodynamics.

In the current study an elongated rectangular cylinder with a chord to thickness (c:t) ratio of 7:1 in a flow of $Re = 3x10^4$ has been evaluated with a commercial CFD code. Experiments were also performed on the cylinder using Particle Image Velocimetry (PIV) and surface pressure measurements. The data presented reveals that there are important differences between the results of the CFD simulations and the experimental data.

2 PRESSURE DATA

The pressure measurements were taken with 24 taps around the periphery of the cylinder. Experimental results are plotted alongside three different numerical simulations in Figure 1 with the tap locations and co-ordinate system shown in Figure 2. The three different simulations were computed using three different turbulence models: the well known k-ε model, the shear stress transport (SST) model and a transient simulation using the SST model. One will note that there is a large discrepancy at taps 3, 4 and 5 located on the bottom of the cylinder (as well as the corresponding taps on top of the cylinder: 21, 22 and 23). These taps are located immediately downstream of the leading corner at $0.12t$, $0.52t$ and $1.32t$, respectively, downstream of the leading corner, where t is the thickness of the cylinder. The greatest concern in this note is with tap 3, 0.12*t* downstream of the corner since the pressure coefficient at this location has the largest difference with the experimental results.

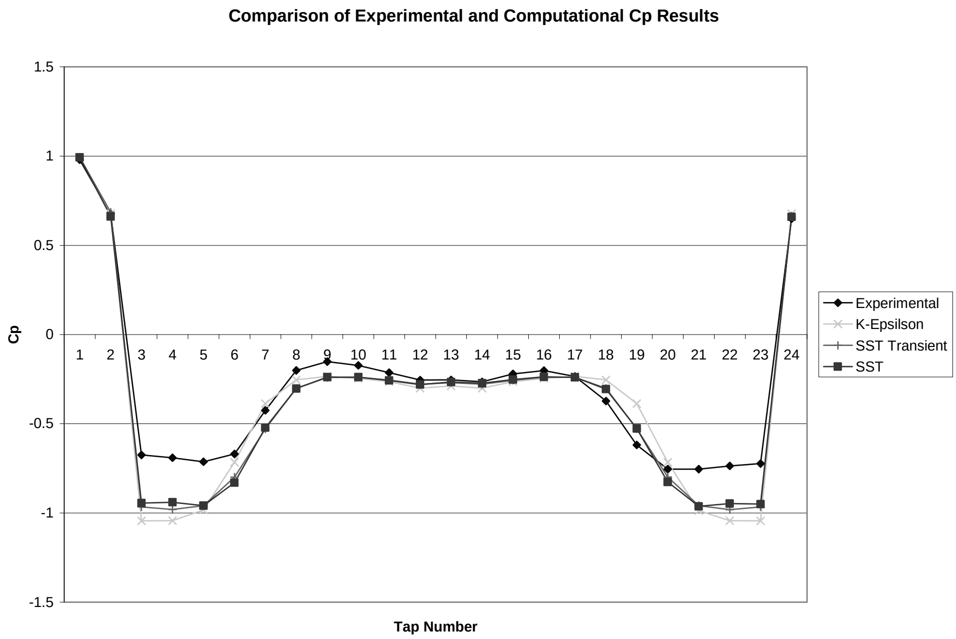

Figure 1. A comparison of experimental pressure data with three different numerical simulations

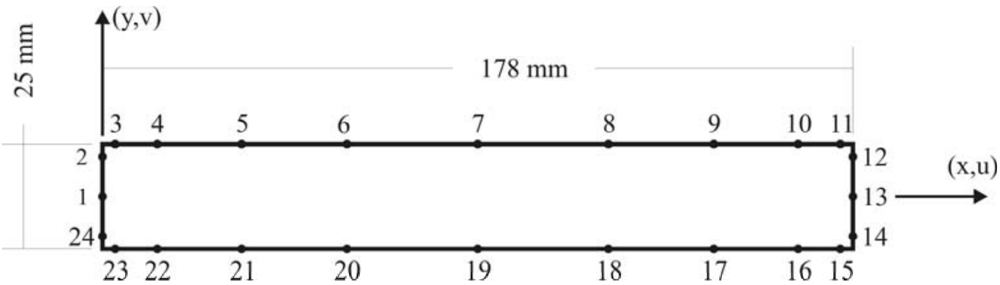

Figure 2. Tap locations for pressure measurements and co-ordinate system

3 VELOCITY DATA

The velocity data were obtained from two PIV experiments, where the only difference between the experiments was the positioning of the camera (i.e., these were two separate experiments). The two different positions allowed for one larger viewing area and one better resolved area.

With PIV data it is possible to plot velocity profiles to compare what is happening in the flow along the bottom of the cylinder with those from the numerical simulations. In Figure 3(a), the velocity profiles at the location of 0.12*t* leeward of the leading edge are plotted. It is observed that there is little reversed flow measured in the PIV experiments whereas in the two CFD results there is indeed a large amount of reversed flow. Figure 3(b) contains the velocity profiles at the first location where significant flow reversal is detected from experiment at 0.16*t* leeward of the leading edge.

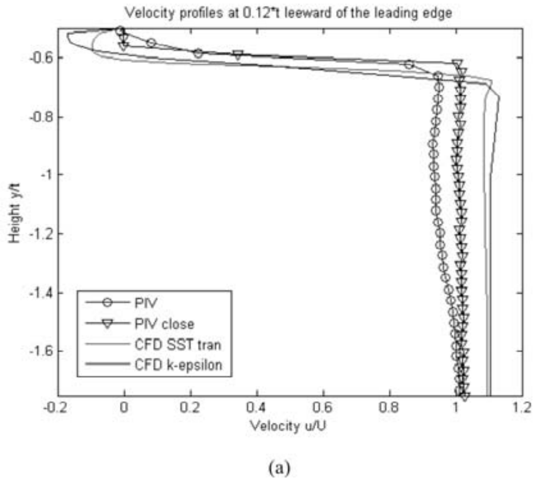

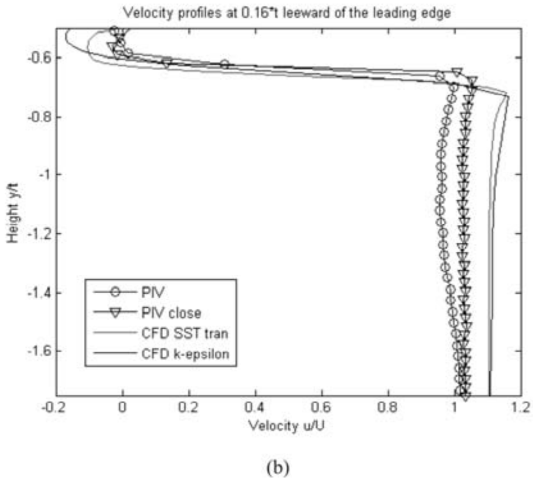

Figure 3. Velocity profiles at (a) 0.12*t* and (b) 0.16*t* leeward of the leading edge.

4 DISCUSSION OF RESULTS

It is apparent from the data presented that there are major differences in the flow between the numerical simulations and the results of both the pressure and PIV experiments. Of particular interest in wind engineering is the difference predicted in the aerodynamic loading, so the difference in the pressure coefficients could be important.

4.1 *Navier-Stokes near the wall*

Using observations of the PIV results via the velocity profiles it is possible to show that the difference in curvature of the velocity profiles will lead to the differences in the pressure coefficients that were observed. The streamwise (x-direction) momentum equation at the wall is:

$$\frac{\partial p}{\partial x} = \mu \frac{\partial^2 u}{\partial y^2} \tag{1}$$

From Equation 1 it is clear that if the velocity profile has a more pronounced flow reversal there will be a greater negative pressure gradient. This agrees with what has been observed in the pressure measurements as the more pronounced flow reversal in the numerical results leads to a greater predicted suction than the experiments reveal. One possible cause of this difference will be examined, namely that the model has a 0.022” radius of curvature at the corners (because of the model construction technique), whereas the numerical modelling has a sharp corner. The effect of this will be examined in the full paper.

4.2 *Hiemenz Flow*

Hiemenz flow, as described in [5], gives an exact solution for a plane stagnation flow and predicts a constant boundary layer thickness along the windward face. It is important to verify that the numerical simulations predict the correct flow on the windward face as the flow at this location will affect the flow further downstream, as separation at the corner is approached. Plotting boundary layer thickness along the windward face (Fig. Figure 4) it is observed that for a large portion of the windward face there exists a constant boundary layer thickness. Thus, it would appear that the CFD is modeling the flow along the windward face correctly.

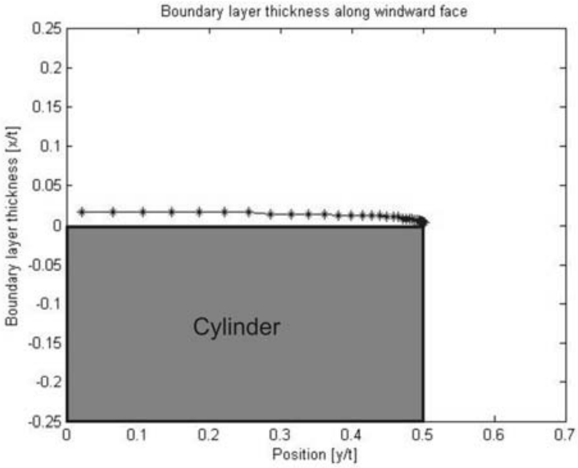

Figure 4. Boundary layer thickness along half of the windward face

5 SUMMARY & DIRECTION

The rectangular cylinder, while quite a simple geometry, is one of great importance in the field of wind engineering. Several differences between the CFD and experimental results were observed around the separation point at the leading edge. Further investigations are underway to determine the causes. It would appear that there are no major differences along the windward face as Hiemenz flow is properly simulated by the numerical methods. Thus, attention now shifts to the leading edge corners as the possible cause of the difference between experiment and numerical simulation. As mentioned above, the edges of the model were not sharp, so modeling of the exact radius of curvature is underway in the CFD simulations to see if this causes the difference in the strength of the separation that was observed. In addition, there is also work underway to investigate the effect that this difference at the leading edge will have on the wake and the overall aerodynamic loads. Both of these aspects will be examined during the full conference presentation.

REFERENCES

1 S. Murakami, Current status and future trends in computational wind engineering, J. Ind. Aerodyn., 67&68 (1997) 3-34.

2 W.A. Dalgliesh and D. Surry, BLWT, CFD and HAM modeling vs. the real world: Bridging the gaps with full-scale measurements, J. Ind. Aerodyn., 91 (2003) 1651-1669.

3 N.J. Cherry, R. Hillier and M.E.M.P. Latour, Unsteady measurements in a separated and reattaching flow, J. Fluid Mech., 144 (1984) 13-46.

4 R. Mills, J. Sheridan and K. Hourigan, Particle image velocimetry and visualization of natural and forced flow around rectangular cylinders, J. Fluid Mech., 478 (2003) 299-323.

5 H. Schlichting and K. Gersten, Boundary Layer Theory: 8th Revised and Enlarged Edition, Springer, Berlin, 2000, p. 110.